HHS Public Access

Author manuscript

Obesity (Silver Spring). Author manuscript; available in PMC 2015 November 15.

Published in final edited form as:

Obesity (Silver Spring). 2011 September ; 19(9): 1735–1741. doi:10.1038/oby.2011.115.

Increased Adipose Protein Carbonylation in Human Obesity

Brigitte I. Frohnert[1], **Alan R. Sinaiko**[2], **Federico J. Serrot**[3], **Rocio E. Foncea**[4], **Antoinette Moran**[1], **Sayeed Ikramuddin**[3], **Umar Choudry**[3], and **David A. Bernlohr**[4]

[1]Division of Pediatric Endocrinology, Department of Pediatrics, University of Minnesota, Minneapolis, Minnesota, USA

[2]Division of Pediatric Nephrology, Department of Pediatrics, University of Minnesota, Minneapolis, Minnesota, USA

[3]Department of Surgery, University of Minnesota, Minneapolis, Minnesota, USA

[4]Department of Biochemistry Molecular Biology and Biophysics, University of Minnesota, Minneapolis, Minnesota, USA

Abstract

Insulin resistance is associated with obesity but mechanisms controlling this relationship in humans are not fully understood. Studies in animal models suggest a linkage between adipose reactive oxygen species (ROS) and insulin resistance. ROS oxidize cellular lipids to produce a variety of lipid hydroperoxides that in turn generate reactive lipid aldehydes that covalently modify cellular proteins in a process termed carbonylation. Mammalian cells defend against reactive lipid aldehydes and protein carbonylation by glutathionylation using glutathione-S-transferase A4 (GSTA4) or carbonyl reduction/oxidation via reductases and/or dehydrogenases. Insulin resistance in mice is linked to ROS production and increased level of protein carbonylation, mitochondrial dysfunction, decreased insulin-stimulated glucose transport, and altered adipokine secretion. To assess protein carbonylation and insulin resistance in humans, eight healthy participants underwent subcutaneous fat biopsy from the periumbilical region for protein analysis and frequently sampled intravenous glucose tolerance testing to measure insulin sensitivity. Soluble proteins from adipose tissue were analyzed using two-dimensional gel electrophoresis and the major carbonylated proteins identified as the adipocyte and epithelial fatty acid–binding proteins. The level of protein carbonylation was directly correlated with adiposity and serum free fatty acids (FFAs). These results suggest that in human obesity oxidative stress is linked to protein carbonylation and such events may contribute to the development of insulin resistance.

INTRODUCTION

The inverse correlation between insulin sensitivity and adiposity is well known (1) and overweight is the single most important predictor of type 2 diabetes mellitus (2). Although

Correspondence: David A. Bernlohr (bernl001@umn.edu).

Disclosure

The authors declared no conflict of interest.

the mechanisms controlling this relationship is not fully understood, substantial evidence exists from animal model systems (3) and human studies to suggest that obesity-related oxidative stress and adipose tissue inflammation may be contributing factors (4,5). Adipose tissue plays an important role in the insulin responsiveness of the whole organism directly through lipolysis and the production of free fatty acid (FFA), increased levels of which are known to potentiate hepatic glucose output, inhibit muscle glucose uptake (6) and indirectly through secretion of adipokines influence insulin sensitivity in liver and muscle (7).

During the development of obesity, expansion of adipose mass has been related to a variety of factors including localized tissue hypoxia, infiltration of inflammatory cells, and alteration in cytokine profile (8–10). Consistent with this, hypoxia in 3T3-L1 adipocytes is associated with inhibition of insulin receptor signaling, increased lipolysis and the induction of reactive oxygen species (ROS) (11). In other experiments, increased levels of ROS in adipocytes have been causally linked to development of insulin resistance in model systems (3).

ROS such as superoxide anion, hydrogen peroxide, and hydroxyl radicals react with a variety of cellular biomolecules leading to modification of intracellular proteins, DNA, RNA, carbohydrates, and lipids. Of the various ROS, hydroxyl radicals are perhaps the most deleterious and lead to the peroxidation of polyunsaturated fatty acyl chains of membrane phospholipids and triglycerides. These peroxidated acyl chains undergo non-enzymatic Hock cleavage forming a family of short and medium chain reactive aldehydes, the most abundant of which are *trans*-4-hydroxy-2-nonenal and *trans*-4-oxo-2-nonenal (12). These reactive aldehydes covalently modify the side chains of histidine, cysteine and lysine residues in a process generically referred to as protein carbonylation. Since the side chains of histidine, lysine and cysteine are frequently components of enzyme active sites or participate in protein–protein interactions, carbonylation commonly leads to loss of function. Moreover, modification frequently targets the proteins for selective degradation by the 26S proteasome (13) leading not only to loss of activity, but also to selective loss of protein. Recent studies in adipose tissue from obese insulin-resistant C57Bl/6J mice have revealed two- to threefold increased levels of total protein carbonylation when compared to lean controls. Among the panel of modified proteins are key factors involved in carbohydrate and lipid metabolism, insulin signaling and a variety of enzymes involved in the antioxidant response (14).

Of the mechanisms used to inactivate reactive lipid species, glutathionylation via glutathione-S-transferase A4 is well studied (15). The expression of glutathione-S-transferase A4 (*GSTA4*) in murine systems is downregulated in part by tumor necrosis factor-α leading to decreased expression in the adipose tissue of high fat fed or genetically obese mice (14,16) while expression levels of other inactivating enzymes such as acetaldehyde dehydrogenase 2 (*ALDH2*) and fatty aldehyde dehydrogenase (*FALDH*) are unchanged (17). Microarray analysis of human subcutaneous adipose tissue (SAT) indicates that *GSTA4* expression was reduced in obese insulin resistant, but not obese insulin sensitive individuals (17) relative to lean controls. Silencing of *GSTA4* in 3T3-L1 adipocytes results in increased total protein carbonylation and multiple metabolic changes including increased basal lipolysis, altered glucose transport, and decreased β-oxidation of fatty acids (13). Both

GSTA4-silenced 3T3-L1 adipocytes and adipose tissue from *GSTA4* knockout mice showed significant impairment in mitochondrial oxidative respiration and increased mitochondrial ROS (17). Other studies in 3T3-L1 adipocytes have shown that insulin receptor substrate-1 and 2 are carbonylated by reactive lipid species leading to reduced insulin-stimulated tyrosine phosphorylation and also targeted degradation (18).

The present study was designed to assess human adipose tissue measures of oxidative stress including protein carbonylation and expression of antioxidant genes and their relationship to body size, body composition and insulin sensitivity. We report herein for the first time protein carbonylation in human adipose tissue is positively correlated with adiposity and serum FFAs.

METHODS AND PROCEDURES

Subjects

This study was approved by the institutional review board of University of Minnesota (Minneapolis, MN) and informed consent was obtained from participants. A total of eight subjects (six men, two women; seven white, one African American) were recruited by letter and telephone call from among a cohort of 357 individuals who had previously participated in a longitudinal study of insulin resistance and cardiovascular risk factors from childhood (age 11–14) into young adulthood, last studied at average age 22 (19,20). From the subjects who responded positively (13 males and 10 females), participants were selected according to availability during the study period. Exclusion criteria included pregnancy and chronic disease. A bariatric surgery patient, not part of the longitudinal study, was recruited only for assessment of visceral adipose tissue (VAT) obtained at the time of bariatric surgery from the omental fat. No subjects were on medications affecting insulin sensitivity.

Clinical measures

Anthropometric measures were obtained by trained research personnel. Body composition was determined by dual energy X-ray absorptiometry with a GE Lunar Prodigy scanner (GE Healthcare Biosciences, Pittsburgh, PA). Abdominal computed tomography at the L4/L5 level was used to measure visceral fat distribution as previously described (21). Venous blood samples were taken after overnight fast for analyses of glucose, insulin and lipids.

Frequently sampled intravenous glucose tolerance test

Following a 10–12 h overnight fast, participants were admitted to the Clinical Research Center. An intravenous catheter was placed in each arm for (i) infusion of a glucose bolus (0.3 g/kg body weight) at time 0 followed by an infusion of insulin (4 mU/kg/min) over 5 min starting at 20 min and (ii) blood samples for plasma glucose and insulin measurements at −10, −1, 2, 4, 8, 19, 22, 30, 40, 50, 70, 90, and 180 min as previously described (22). The data were analyzed according to the minimal model, using the computer program MINMOD to generate insulin sensitivity index (SI), glucose disposition index (DI) and the acute insulin response to glucose (23,24).

Adipose tissue sampling

Under standard sterile technique and local anesthesia (1% lidocaine with epinephrine), a curvilinear ellipse of skin along with the underlying adipose tissue was excised from the inferior periumbilical abdominal area and a total of 2–5 g of fat was obtained from each subject. The specimens were dissected to remove stromal tissue, immediately frozen with liquid nitrogen in aliquots of 0.1–0.2 g, and stored at −70 °C until further study.

Analysis of protein carbonylation

To evaluate protein carbonylation, adipose tissue was minced and homogenized on ice in coupling buffer (100 mmol/l sodium acetate at pH 5.5, 20 mmol/l NaCl and 0.1 mmol/l EDTA supplemented with 0.1 mmol/l phenylmethanesulfonyl fluoride, 2 mg/ml pepstatin, 2 mg/ml aprotinin, 2 mg/ml leupeptin). Homogenates were centrifuged at 600*g* at 4 °C for 5 min to separate the lipid cake, the infranatant was removed and sodium dodecyl sulfate (SDS; Sigma-Aldrich, St Louis, MO) was added to a final concentration of 1%. The lysate was centrifuged at 100,000*g* for 1 h at 4 °C to remove insoluble residue and the supernatant recovered and assayed for protein content (BCA assay; Sigma-Aldrich). A total of 25 μg of soluble protein was coupled with EZ-link biotin hydrazide (Pierce Biotechnology, Rockford, IL) to covalently label free aldehydes as previously (14) described. Proteins were separated by SDS-polyacrylamide gel electrophoresis (10–20% acrylamide gradient gel), transferred to polyvinylidene fluoride (Millipore, Billerica, MA) membranes and blocked in Odyssey Blocking Buffer (Li-Cor, Lincoln, NE). Biotinylated proteins were detected with DyLight 800 Conjugated Streptavidin (Pierce). As a loading control, the biotin hydrazide blot was probed with mouse anti β-actin antibody and IRDye 680 conjugated goat (polyclonal) anti-mouse secondary antibody. Biotinylated proteins and β-actin loading control bands were visualized using a LiCor Odyssey Infrared Imager. Both total protein carbonylation as well as intensity of the β-actin band were determined by quantification of LiCor signal intensity. Protein carbonylation is reported normalized to β-actin band.

Two-dimensional gel electrophoresis

Total soluble protein was isolated from the visceral fat sample and coupled with biotin hydrazide. One hundred micrograms of sample was allowed to rehydrate into a 13 cm Immobline DryStrip, pH 3–10 (GE Healthcare) overnight. After overnight rehydration, the Immobline DryStrip sample was resolved with an Ettan IPGphor IEF apparatus (Amersham (GE Healthcare), Waukesha, WI) until a total 19.255 kVh was reached. The IEF strip was equilibrated for 0.5 h in SDS equilibration buffer (50 mmol/l Tris, pH 8.8, 8 mol/l urea, 30% glycerol, 4% SDS, 1% dithiothreitol (Sigma-Aldrich) followed by separation on 10–20% Tris-HCl SDS-PAGE Criterion gel (BioRad). After SDS-polyacrylamide gel electrophoresis, the gel was stained with Deep Purple total protein stain (GE Healthcare) according to the manufacturer's instructions. The gel image was visualized with the Typhoon 8610 scanner (GE Healthcare). Separated protein from parallel gels were transferred to polyvinylidene fluoride membranes and probed for carbonylated proteins with IR800-streptavidin as described. Additionally, membranes were incubated with either rabbit anti-mouse A-FABP polyclonal antibody or rabbit anti-mouse E-FABP polyclonal antibody at 1:10,000 dilution at 4 °C overnight. Membranes were washed with phosphate-buffered

saline containing 0.05% Tween (phosphate-buffered saline tween) and incubated for 1 h with IR-680 goat anti-rabbit secondary antibody at 1:10,000 and scanned using an Odyssey Infrared Imager in both the 700 nm and 800 nm channels.

RNA extraction, reverse transcription and real-time PCR

Total RNA was extracted from about 0.2 g of adipose tissue using Trizol (Invitrogen, Carlsbad, CA) according to the manufacturer's instructions. After DNase treatment, cDNA was synthesized using iScript cDNA synthesis kit (BioRad, Hercules, CA). Relative quantification of mRNAs was performed by real-time PCR using iQ SYBR green Supermix and the MyiQ detection system (BioRad). Primers for the target genes were *hGSTA4*: forward 5′-GGA GTC CGT GAG ATG GGT TTT AG-3′ and reverse 5′-TGC TAT GTA GTG GAG AAT GCT TCG-3′; *hALDH2*: forward 5′-CACTTCGCCCTGTTCTTCAACC-3′ and reverse 5′-CC TGCTCGGTCTTGCTATCAAAG-3′; *hFALDH*: forward 5′-TACGG GAAACACTGCGGTTG-3′ and reverse 5′-GCAAACAATGTCCA GGTCACAATC-3′; and the reference gene TATA binding protein: forward 5′-AGC GGT TTG CTG CGG TAA TC-3′ and reverse 5′-ACT GTT CTT CAC TCT TGG CTC CTG-3′. All primers were validated in human subcutaneous and VAT, using TATA binding protein as the reference gene.

Data analysis

All comparisons were done using Pearson's correlations. Statistical analyses were conducted using the statistical package SAS, version 9.2 for Windows (SAS Institute, Cary, NC).

RESULTS

Subject characteristics

There was a narrow age range (25–27 years), but a broad range in BMI, with two subjects of normal weight (BMI <25), three were overweight (BMI 25–30), and three with BMI measurements greater than 40 kg/m^2 (Table 1). None had diabetes and none had impaired fasting glucose (≥100 mg/dl) as defined by the American Diabetes Association (25). The subjects exhibited a wide range of fasting insulin, acute insulin response to glucose, Sg (glucose mediated glucose uptake), SI and DI. Characteristics for men and women in the study were similar, with the exception of the ratio of VAT to SAT, which was significantly higher in males relative to females (0.39 ± 0.07 vs. 0.24 ± 0.03, $P = 0.031$), and serum high-density lipoprotein which was significantly higher in females relative to males (58 ± 3 vs. 37 ± 8, $P = 0.012$).

There were strong trends for an inverse correlation between SI and BMI ($r = -0.54$), VAT ($r = -0.71$) and SAT ($r = -0.59$) (Figure 1), but only the correlation with visceral adiposity was significant ($P = 0.028$) most likely due to the small sample size. DI was inversely related to BMI ($r = -0.53$, $P = 0.17$) and FFA levels ($r = -0.83$, $P = 0.011$).

Carbonylation profile of adipose tissue protein

Figure 2a shows the profile of total soluble proteins in adipose tissue separated by both mass (vertically) and isoelectric point (horizontally). Figure 2b,d shows the subset of carbonylated

adipose proteins with a prominent species noted at about 67 kDa, likely representing albumin, as well as multiple species at about 15 kDa. Two members of the fatty acid–binding protein multigene family are expressed in adipose tissue: adipocyte fatty acid–binding protein (A-FABP) found primarily in adipocytes, and epidermal fatty acid–binding protein (E-FABP) expressed abundantly in macrophages. Both A-FABP and E-FABP are carbonylated in murine adipose tissue suggesting that the 15 kDa human carbonylated proteins may be FABPs. In order to verify the identity of the carbonylated 15 kDa proteins, the membranes were immunoblotted with anti–A-FABP or anti–E-FABP antibodies (Figure 2c,e). The FABP immunoreactive protein exactly matched the 15 kDa carbonylated protein indicating that both A-FABP and E-FABP are carbonylated in human adipose tissue and that multiple charged species for each protein are modified.

Carbonylation of adipose proteins from study subjects

Figure 3a shows a representative blot from one lean and one obese individual where the fatty acid–binding protein band is denoted by an arrow. For each individual, total carbonylation was quantified by analysis of the signal intensity for the entire lane. There was a highly significant positive correlation between total protein carbonylation and BMI ($r = 0.86$, $P = 0.0067$) (Figure 3b), VAT ($r = 0.71$, $P = 0.048$) and SAT ($r = 0.84$, $P = 0.0098$). When carbonylation was measured excluding the 67 kDa albumin band, these relationships were essentially unchanged, with significant positive correlations between carbonylation and BMI ($r = 0.85$, $P = 0.0080$), VAT ($r = 0.74$, $P = 0.036$) and SAT ($r = 0.83$, $P = 0.010$).

Relationship of carbonylation to metabolic parameters

Total carbonylation was significantly related to FFA ($r = 0.77$, $P = 0.025$) (Figure 4) and remained significant after adjusting for visceral adiposity ($r = 0.80$, $P = 0.033$) and VAT/SAT ratio ($r = 0.76$, $P = 0.048$); however the correlation was slightly attenuated and non-significant after adjusting for BMI ($r = 0.66$, $P = 0.11$). Fasting insulin also was significantly related to carbonylation ($r = 0.74$, $P = 0.034$). It was significant after adjusting for VAT/SAT ratio ($r = 0.85$, $P = 0.014$) but was no longer significant after adjusting for visceral adiposity ($r = 0.32$, $P = 0.49$) or BMI ($r = -0.01$, $P = 0.98$). As seen in Figure 5, the relationship of total carbonylation to DI and SI showed a negative trend but was not statistically significant ($r = -0.58$, $P = 0.13$ and. $r = -0.34$, $P = 0.42$, respectively). The relationship of DI to total carbonylation became more significant when adjusted for the ratio of visceral to SAT volume ($r = -0.67$, $P = 0.099$).

Expression of antioxidant genes involved in reactive aldehyde metabolism

The expression of *GSTA4*, *ALDH2* and *FALDH*, three enzymes linked to oxidative stress and reactive aldehyde metabolism were strongly related to each other and were related to measures of adiposity (Table 2). *FALDH* significantly correlated with BMI ($r = 0.67$) and % body fat ($r = 0.59$). *ALDH2* was significantly correlated with % body fat ($r = 0.73$). *GSTA4* was not significantly correlated with any of the three measures of body fatness. The expression of *GSTA4*, *ALDH2* or *FALDH* was not significantly related to carbonylation (Table 3).

DISCUSSION

Obesity is associated with an increase in inflammation and oxidative stress in adipose tissue (26). Oxidative stress-induced lipid peroxidation results in production of reactive aldehydes that diffuse within cells and across membranes to covalently modify the side chains of histidine, lysine and cysteine residues, a process known as protein carbonylation. Studies in mice have shown that the level of carbonylation is significantly associated with obesity and insulin resistance. The present study shows for the first time the relationship of carbonylation to obesity in humans and demonstrates that multiple protein targets are modified by reactive aldehydes in human adipose tissue and carbonylation occurs to a greater degree in the adipose tissue of obese relative to lean individuals. Moreover, protein carbonylation is strongly related to serum FFA levels, even after adjusting for adiposity. Although not statistically significant, the study also showed r values of −0.34 and −0.58 between carbonylation and DI and SI, respectively, suggesting the need for studies conducted in a larger number of subjects. It should be noted that carbonylation does not necessarily imply a pathogenic process. Increased carbonylation in adipocytes might represent a homeostatic response to increased adipocyte fat and oxidative stress limiting nutrient influx to large cells and diverting carbohydrates and lipids to smaller adipocytes.

As shown in Figure 2, a wide variety of adipose proteins are carbonylated suggesting that modification may result in alteration of multiple metabolic processes. Moreover, since the extent of carbonylation on any one specific target protein is not likely to be stoichiometric, changes in metabolism or signaling are likely to be the result of multiple small changes common to a pathway or process. For example, in aged rat muscle mitochondria (27) carbonylation was detected in multiple enzymes of the electron transport system and even within a particular complex. Multiple carbonylation events on targets within a single pathway, even if each is sub-stoichiometric, may be sufficient to alter overall metabolic flux and/or function. This may be particularly true of targets that are rate-limiting enzymes or regulatory (e.g., protein kinases or phosphatases) in nature.

In humans, defects of mitochondrial metabolism in subcutaneous and VAT have been associated with insulin resistance (28,29). It is known that production of ROS by mitochondria inhibits the proliferation of preadipocytes without inducing apoptosis (reviewed in ref. 30). This could lead to adipocyte hypertrophy resulting in larger, dysfunctional fat cells. Carbonylation may also lead to decreased mitochondrial biogenesis as evidenced by changes in key factors in adipocytes at both the mRNA and protein levels (17) or there may be direct carbonylation of mitochondrial proteins, causing dysfunction or targeting for degradation.

Increased adipose protein carbonylation has been associated with impaired insulin signaling (18) and increased lipolysis in cell culture models (17). Consistent with this, in this study there was a positive association of carbonylation with serum FFA levels that persisted after adjustment for adiposity. Elevated serum FFAs are associated with both peripheral insulin resistance as well as impaired β-cell function in humans (26,31). A-FABP and E-FABP, proteins that mediate lipolysis in adipocytes (14,32), were identified by this study as carbonylation targets in human adipose tissue. Modification of both fatty acid–binding

proteins has been shown in mice to occur at a conserved cysteine residue that lies within the lipidbinding cavity (32,33). This cysteine residue is also conserved in human A-FABP (34) and occupation of the lipid-binding site by *trans*-4-hydroxy-2-nonenal may affect lipolytic rate (14). Beyond lipolysis, there are other potential reasons why carbonylation of FABPs may affect cellular function. As some of the most abundant proteins in adipose tissue, FABPs may play an important role as a scavenger for the reactive aldehyde products of oxidative stress, sequestering them and removing the reactive lipids from the cell. In addition, A-FABP is known to interact with other metabolically important adipocyte proteins, such as hormone sensitive lipase and peroxisome proliferator-activated receptor-γ (31,32). It should be noted that these studies are of whole adipose tissue that consists of inflammatory macrophages, T-cells, stromal-vascular cells and preadipocytes in addition to mature adipocytes. A-FABP is primarily adipocyte in origin while E-FABP is expressed more highly in macrophages. Further study will be needed to determine whether carbonylation is playing an important role in the various cell types found in adipose tissue.

Increased intracellular oxidative stress, possibly related to localized tissue hypoxia, occurs in the adipose tissue of obese individuals (26). The increased levels of ROS likely reflect production of ROS by NADPH oxidase and/or the mitochondria as well as decreased detoxification of ROS by the antioxidant enzyme system. In the present study, the expression of three antioxidant genes, *GSTA4*, *ALDH2* and *FALDH*, was investigated with the expectation that decreased expression of some or all of these genes would be associated with increased carbonylation as was previously reported in mouse and cell culture studies (13,14). Although there was no significant change in *GSTA4* expression with increasing adiposity, the expression of both *ALDH2* and *FALDH* increased with fat mass, possibly representing a counter-regulatory response to increased lipid aldehyde production. However, none of the three was strongly associated with total carbonylation level despite being previously shown to be inversely related to insulin resistance and carbonylation in animal model systems (18,35,36). It should be noted however that none of the patients in the study had diabetes or impaired fasting glucose. While all three enzymes have antioxidant functions, their regulation may be quite different, making simple associations in humans difficult. For example, *FALDH*, but not *GSTA4* or *ALDH2*, is upregulated by insulin (36).

In summary, the results show for the first time in humans that protein carbonylation in adipose tissue is directly related to BMI and is directly related to serum free fatty levels. These findings are in concert with prior studies in animal models that suggest protein carbonylation is associated with adipose mitochondrial dysfunction and insulin resistance. Further studies will be needed to determine whether there is a significant relationship between carbonylation and disposition index and insulin sensitivity. Additionally, the identification of carbonylation targets and their regulation by oxidative stress may further elucidate the role of this process in obesity-related adipose dysfunction.

ACKNOWLEDGMENTS

This work was supported by National Institute of Health Grants DK084669 (to D.A.B.) and HL52851 (to A.R.S.), the Minnesota Obesity Center (NIH DK050456) and Vikings Pediatric Fellow's Grant (to B.I.F.). We thank Lori Schafer for her invaluable work in study coordination. We thank the members of the Bernlohr laboratory for helpful

comments and suggestions during the preparation of this manuscript. We also thank Todd Markowski at the Center for Mass Spectrometry and Proteomics and the University of Minnesota Supercomputing Institute.

REFERENCES

1. DeFronzo RA, Bonadonna RC, Ferrannini E. Pathogenesis of NIDDM. A balanced overview. Diabetes Care. 1992; 15:318–368. [PubMed: 1532777]
2. Hu FB, Manson JE, Stampfer MJ, et al. Diet, lifestyle, and the risk of type 2 diabetes mellitus in women. N Engl J Med. 2001; 345:790–797. [PubMed: 11556298]
3. Houstis N, Rosen ED, Lander ES. Reactive oxygen species have a causal role in multiple forms of insulin resistance. Nature. 2006; 440:944–948. [PubMed: 16612386]
4. Sinaiko AR, Steinberger J, Moran A, et al. Relation of body mass index and insulin resistance to cardiovascular risk factors, inflammatory factors, and oxidative stress during adolescence. Circulation. 2005; 111:1985–1991. [PubMed: 15837953]
5. Steffes MW, Gross MD, Lee DH, Schreiner PJ, Jacobs DR Jr. Adiponectin, visceral fat, oxidative stress, and early macrovascular disease: the Coronary Artery Risk Development in Young Adults Study. Obesity (Silver Spring). 2006; 14:319–326. [PubMed: 16571859]
6. Abdul-Ghani MA, DeFronzo RA. Pathogenesis of insulin resistance in skeletal muscle. J Biomed Biotechnol. 2010; 2010:476279. [PubMed: 20445742]
7. Bays H, Mandarino L, DeFronzo RA. Role of the adipocyte, free fatty acids, and ectopic fat in pathogenesis of type 2 diabetes mellitus: peroxisomal proliferator-activated receptor agonists provide a rational therapeutic approach. J Clin Endocrinol Metab. 2004; 89:463–478. [PubMed: 14764748]
8. Ye J, Gao Z, Yin J, He Q. Hypoxia is a potential risk factor for chronic inflammation and adiponectin reduction in adipose tissue of ob/ob and dietary obese mice. Am J Physiol Endocrinol Metab. 2007; 293:E1118–E1128. [PubMed: 17666485]
9. Rausch ME, Weisberg S, Vardhana P, Tortoriello DV. Obesity in C57BL/6J mice is characterized by adipose tissue hypoxia and cytotoxic T-cell infiltration. Int J Obes (Lond). 2008; 32:451–463. [PubMed: 17895881]
10. Hosogai N, Fukuhara A, Oshima K, et al. Adipose tissue hypoxia in obesity and its impact on adipocytokine dysregulation. Diabetes. 2007; 56:901–911. [PubMed: 17395738]
11. Trayhurn P, Wood IS. Adipokines: inflammation and the pleiotropic role of white adipose tissue. Br J Nutr. 2004; 92:347–355. [PubMed: 15469638]
12. Sayre LM, Lin D, Yuan Q, Zhu X, Tang X. Protein adducts generated from products of lipid oxidation: focus on HNE and one. Drug Metab Rev. 2006; 38:651–675. [PubMed: 17145694]
13. Carini M, Aldini G, Facino RM. Mass spectrometry for detection of 4-hydroxy-trans-2-nonenal (HNE) adducts with peptides and proteins. Mass Spectrom Rev. 2004; 23:281–305. [PubMed: 15133838]
14. Grimsrud PA, Picklo MJ Sr, Griffin TJ, Bernlohr DA. Carbonylation of adipose proteins in obesity and insulin resistance: identification of adipocyte fatty acid-binding protein as a cellular target of 4-hydroxynonenal. Mol Cell Proteomics. 2007; 6:624–637. [PubMed: 17205980]
15. Hubatsch I, Ridderström M, Mannervik B. Human glutathione transferase A4-4: an alpha class enzyme with high catalytic efficiency in the conjugation of 4-hydroxynonenal and other genotoxic products of lipid peroxidation. Biochem J. 1998; 330(Pt 1):175–179. [PubMed: 9461507]
16. Moraes RC, Blondet A, Birkenkamp-Demtroeder K, et al. Study of the alteration of gene expression in adipose tissue of diet-induced obese mice by microarray and reverse transcription-polymerase chain reaction analyses. Endocrinology. 2003; 144:4773–4782. [PubMed: 12960083]
17. Curtis JM, Grimsrud PA, Wright WS, et al. Downregulation of adipose glutathione S-transferase A4 leads to increased protein carbonylation, oxidative stress, and mitochondrial dysfunction. Diabetes. 2010; 59:1132–1142. [PubMed: 20150287]
18. Demozay D, Mas JC, Rocchi S, Van Obberghen E. FALDH reverses the deleterious action of oxidative stress induced by lipid peroxidation product 4-hydroxynonenal on insulin signaling in 3T3-L1 adipocytes. Diabetes. 2008; 57:1216–1226. [PubMed: 18174527]

19. Moran A, Jacobs DR Jr, Steinberger J, et al. Insulin resistance during puberty: results from clamp studies in 357 children. Diabetes. 1999; 48:2039–2044. [PubMed: 10512371]
20. Sinaiko AR, Jacobs DR Jr, Steinberger J, et al. Insulin resistance syndrome in childhood: associations of the euglycemic insulin clamp and fasting insulin with fatness and other risk factors. J Pediatr. 2001; 139:700–707. [PubMed: 11713450]
21. van der Kooy K, Seidell JC. Techniques for the measurement of visceral fat: a practical guide. Int J Obes Relat Metab Disord. 1993; 17:187–196. [PubMed: 8387967]
22. Steil GM, Volund A, Kahn SE, Bergman RN. Reduced sample number for calculation of insulin sensitivity and glucose effectiveness from the minimal model. Suitability for use in population studies. Diabetes. 1993; 42:250–256. [PubMed: 8425661]
23. Muniyappa R, Lee S, Chen H, Quon MJ. Current approaches for assessing insulin sensitivity and resistance in vivo: advantages, limitations, and appropriate usage. Am J Physiol Endocrinol Metab. 2008; 294:E15–E26. [PubMed: 17957034]
24. Pacini G, Bergman RN. MINMOD: a computer program to calculate insulin sensitivity and pancreatic responsivity from the frequently sampled intravenous glucose tolerance test. Comput Methods Programs Biomed. 1986; 23:113–122. [PubMed: 3640682]
25. Genuth S, Alberti KG, Bennett P, et al. Expert Committee on the Diagnosis and Classification of Diabetes Mellitus. Follow-up report on the diagnosis of diabetes mellitus. Diabetes Care. 2003; 26:3160–3167. [PubMed: 14578255]
26. de Ferranti S, Mozaffarian D. The perfect storm: obesity, adipocyte dysfunction, and metabolic consequences. Clin Chem. 2008; 54:945–955. [PubMed: 18436717]
27. Meany DL, Xie H, Thompson LV, Arriaga EA, Griffin TJ. Identification of carbonylated proteins from enriched rat skeletal muscle mitochondria using affinity chromatography-stable isotope labeling and tandem mass spectrometry. Proteomics. 2007; 7:1150–1163. [PubMed: 17390297]
28. Sears DD, Hsiao G, Hsiao A, et al. Mechanisms of human insulin resistance and thiazolidinedione-mediated insulin sensitization. Proc Natl Acad Sci USA. 2009; 106:18745–18750. [PubMed: 19841271]
29. Dahlman I, Forsgren M, Sjögren A, et al. Downregulation of electron transport chain genes in visceral adipose tissue in type 2 diabetes independent of obesity and possibly involving tumor necrosis factor-alpha. Diabetes. 2006; 55:1792–1799. [PubMed: 16731844]
30. De Pauw A, Tejerina S, Raes M, Keijer J, Arnould T. Mitochondrial (dys) function in adipocyte (de)differentiation and systemic metabolic alterations. Am J Pathol. 2009; 175:927–939. [PubMed: 19700756]
31. Schaffer JE. Lipotoxicity: when tissues overeat. Curr Opin Lipidol. 2003; 14:281–287. [PubMed: 12840659]
32. Bennaars-Eiden A, Higgins L, Hertzel AV, et al. Covalent modification of epithelial fatty acid-binding protein by 4-hydroxynonenal *in vitro* and *in vivo*. Evidence for a role in antioxidant biology. J Biol Chem. 2002; 277:50693–50702. [PubMed: 12386159]
33. Hellberg K, Grimsrud PA, Kruse AC, et al. X-ray crystallographic analysis of adipocyte fatty acid binding protein (aP2) modified with 4-hydroxy-2- nonenal. Protein Sci. 2010; 19:1480–1489. [PubMed: 20509169]
34. Baxa CA, Sha RS, Buelt MK, et al. Human adipocyte lipid-binding protein: purification of the protein and cloning of its complementary DNA. Biochemistry. 1989; 28:8683–8690. [PubMed: 2481498]
35. Xu F, Chen Y, Lv R, et al. ALDH2 genetic polymorphism and the risk of type II diabetes mellitus in CAD patients. Hypertens Res. 2010; 33:49–55. [PubMed: 19876063]
36. Demozay D, Rocchi S, Mas JC, et al. Fatty aldehyde dehydrogenase: potential role in oxidative stress protection and regulation of its gene expression by insulin. J Biol Chem. 2004; 279:6261–6270. [PubMed: 14638678]

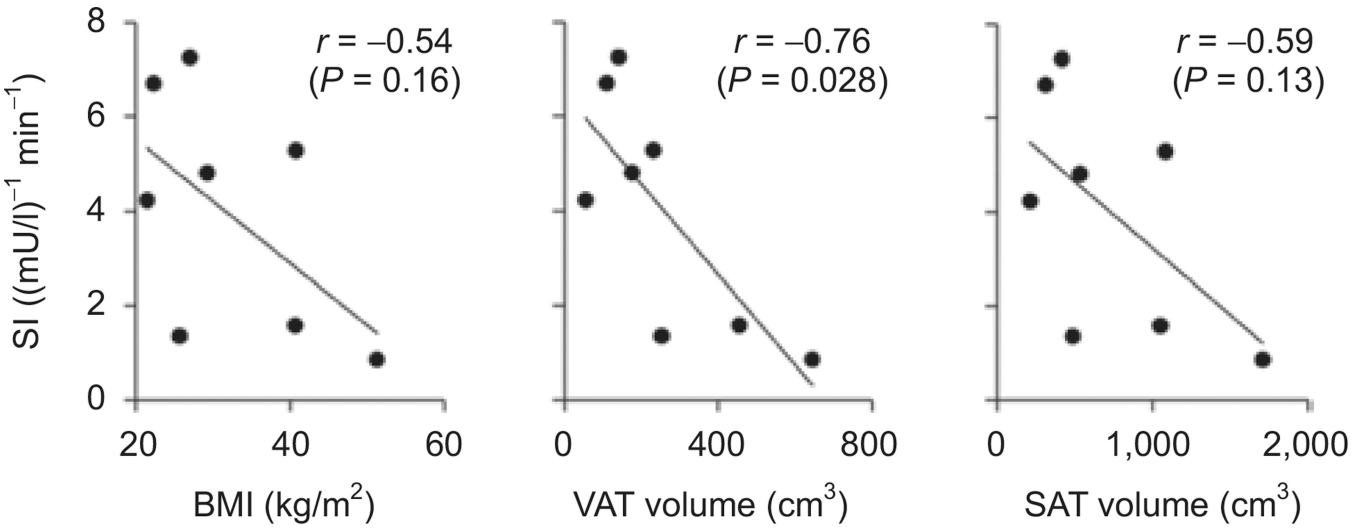

Figure 1.

Sensitivity index correlates negatively with BMI, visceral, and subcutaneous fat volume. Visceral adipose tissue (VAT) and subcutaneous adipose tissue (SAT) volumes determined by single-slice CT at midabdomen (level of L2–L4). Pearson's correlation (*r*) and *P* value are indicated for each graph.

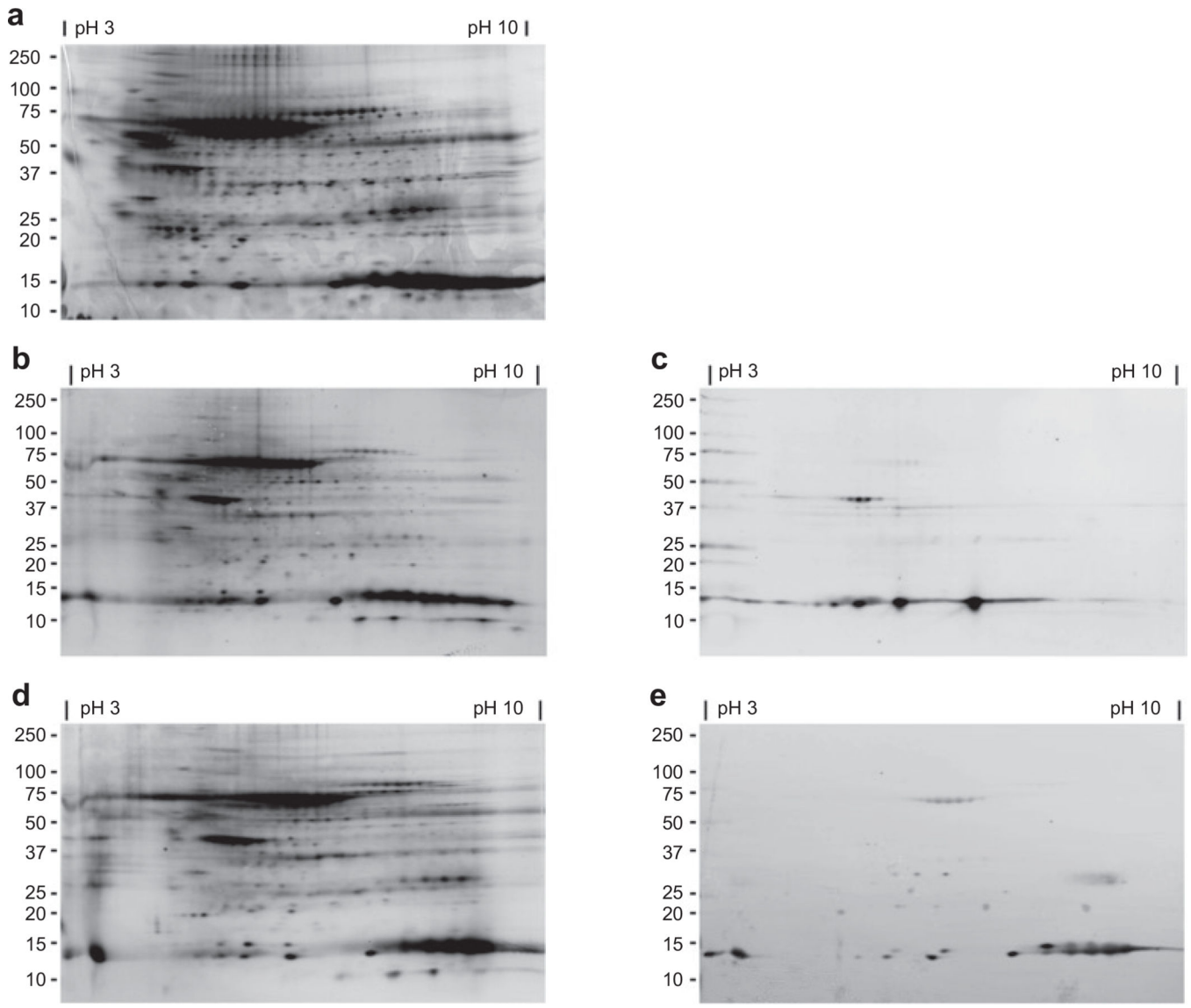

Figure 2.

Two-dimension gel electrophoresis of total soluble protein from human visceral fat. All blots and gel have molecular weight in kilodaltons (kDa) noted along left hand side and pH of range of isoelectric focusing is noted along the top. (**a**) Total soluble protein stained with Deep Purple. (**b**) Total carbonylated protein and corresponding immunoblot (**c**) using anti–A-FABP antibody. (**d**) Total carbonylated protein and corresponding immunoblot (**e**) using anti–E-FABP antibody. A-FABP, adipocyte fatty acid–binding protein; E-FABP, epidermal fatty acid–binding protein.

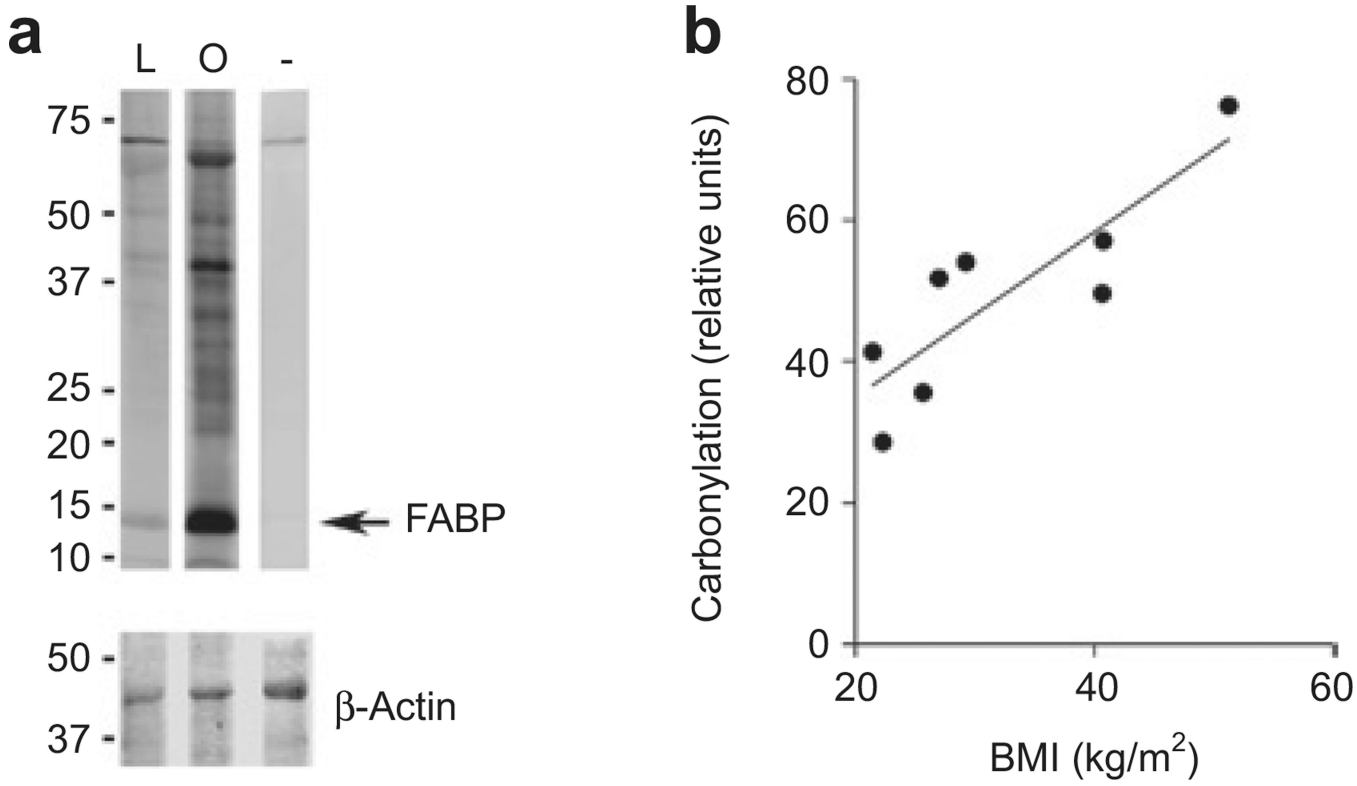

Figure 3.

Carbonylation correlates positively with adiposity. (**a**) Carbonylation of total soluble proteins (upper panel) from a representative lean individual (L) and obese individual (O). Negative control is shown on the right (−). Molecular masses (kDa) of proteins are indicated on the left. The same membrane was blotted for β-actin (lower panel) as a loading control. Image shown is from the same gel taken at the same exposure but composed from lanes not adjacent to each other. (**b**) Total carbonylated protein was quantified for each individual, normalized to β-actin and plotted relative to BMI (kg/m^2). FABP, fatty acid–binding protein.

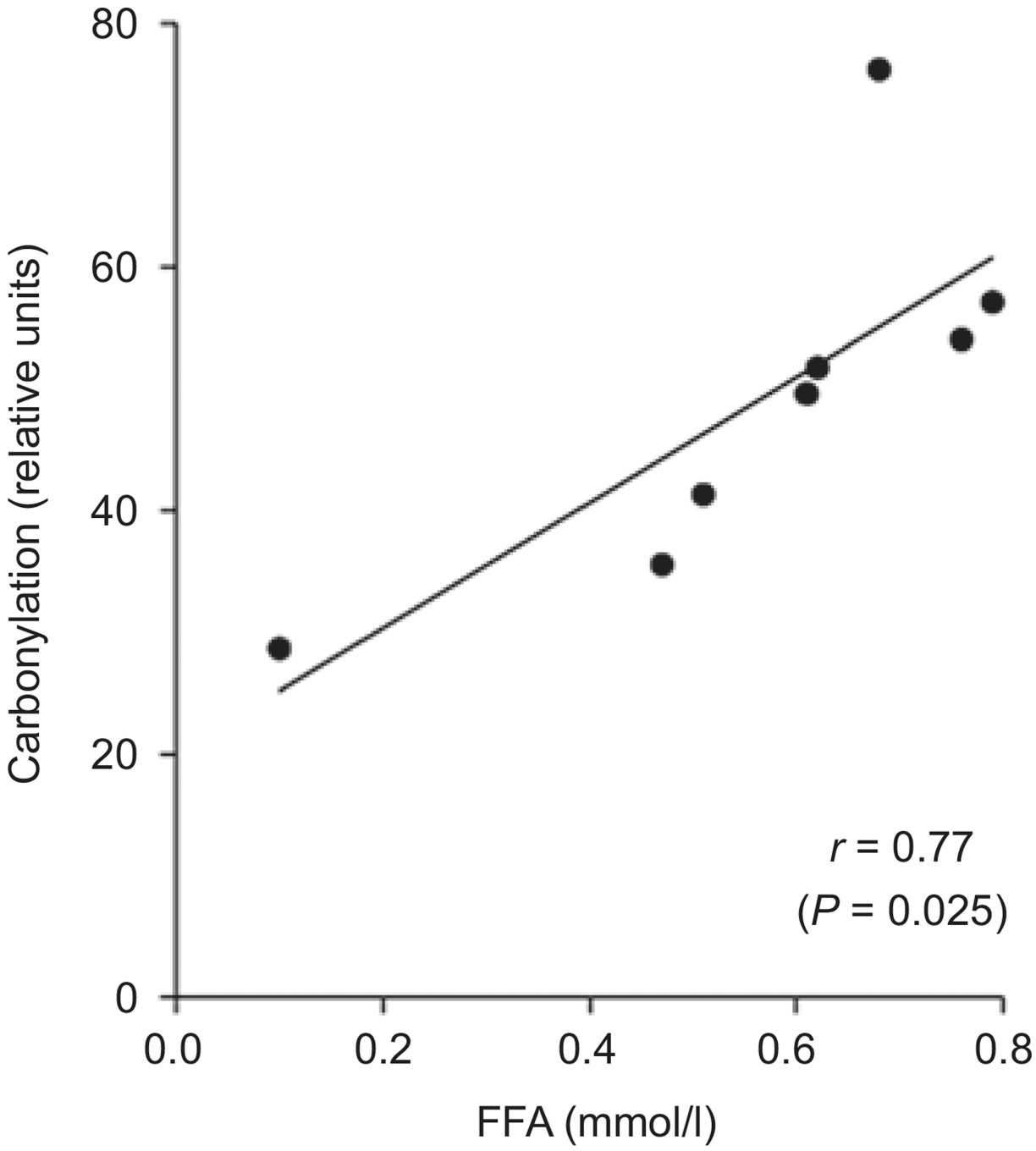

Figure 4.
Relationship of protein carbonylation to serum free fatty acid (FFA) levels. Total protein carbonylation was quantified for each individual, normalized to β-actin, and plotted relative to serum FFA (mmol/l).

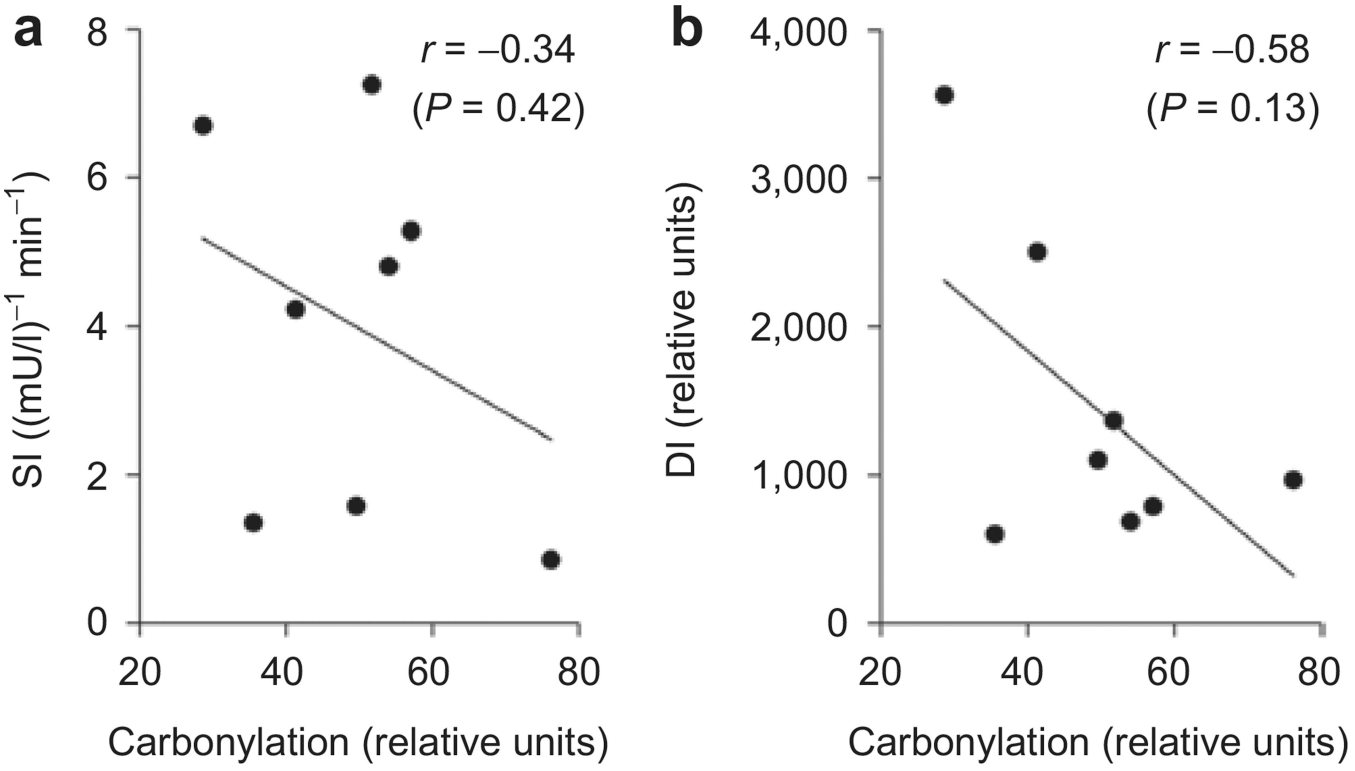

Figure 5.

Relationship of protein carbonylation to insulin sensitivity. Total protein carbonylation was quantified for each individual, normalized to β-actin, and plotted relative to (**a**) insulin sensitivity index (SI) and (**b**) disposition index (DI). Pearson's correlation *r* and *P* value are indicated for each graph.

Table 1

Subject characteristics, mean ± s.d.

Clinical characteristics	All (n = 8)	Females (n = 2)	Males (n = 6)	Range
Age (years)	26 ± 1	26 ± 1	26 ± 1	25–27
BMI (kg/m^2)	32 ± 11	31 ± 14	33 ± 11	22–51
Body fat (%)	35 ± 14	41 ± 25	33 ± 11	20–59
VAT volume (cm^3)	258 ± 197	142 ± 124	296 ± 210	55–645
SAT volume (cm^3)	724 ± 510	647 ± 616	750 ± 534	211–1,708
VAT/SAT ratio	0.34 ± 0.10	0.24 ± 0.03[a]	0.39 ± 0.07[a]	0.21–0.52
Cholesterol (mg/dl)	168 ± 43	178 ± 47	165 ± 46	110–232
LDL (mg/dl)	105 ± 39	100 ± 36	107 ± 43	51–168
HDL (mg/dl)	42 ± 12	58 ± 3[a]	37 ± 8[a]	27–60
Triglycerides (mg/dl)	103 ± 37	98 ± 45	104 ± 39	62–163
FFA (mmol/l)	0.57 ± 0.22	0.65 ± 0.20	0.54 ± 0.24	0.10–0.79
SBP (mm Hg)	118 ± 16	107 ± 9	121 ± 16	101–152
DBP (mm Hg)	68 ± 13	63 ± 12	69 ± 14	54–93
Fasting glucose (mg/dl)	88 ± 3	86 ± 3	89 ± 3	84–93
Fasting insulin (mU/l)	7.0 ± 5.0	4.5 ± 1.4	7.8 ± 5.6	3–18
AIRg (mU/l/min)	490 ± 340	370 ± 310	520 ± 360	140–1,130
SI (min·mU/l)$^{-1}$	4.0 ± 2.5	4.7 ± 0.7	3.8 ± 2.9	0.8–7.3
Sg (min^{-1})	0.020 ± 0.007	0.024 ± 0.001	0.018 ± 0.008	0.004–0.028
DI	1,450 ± 1,050	1650 ± 1210	1380 ± 1200	605–3,560

AIRg, acute insulin response to glucose; DBP, diastolic blood pressure; DI, disposition index; FFA, free fatty acid; HDL, high-density lipoprotein; LDL, low-density lipoprotein; SAT, subcutaneous adipose tissue; SBP, systolic blood pressure; Sg, glucose effectiveness; SI, sensitivity index; VAT, visceral adipose tissue.

[a]Denotes significant difference between female and male subjects ($P < 0.05$).

Table 2

Pearson's coefficients of correlation between gene expression and BMI, visceral adipose tissue (VAT) volume and total body fat

Gene	BMI	VAT volume (cm^3)	% Body fat
GSTA4	0.25	−0.07	0.59
ALDH2	0.57	0.36	0.73*
FALDH	0.67*	0.45	0.83**

ALDH2, acetaldehyde dehydrogenase 2; FALDH, fatty aldehyde dehydrogenase; GSTA4, glutathione S-transferase A4.

*$P < 0.10$,

**$P < 0.05$.

Table 3

Pearson's coefficients of correlation between carbonylation and expression of antioxidant genes

	GSTA4	ALDH2	FALDH
Total carbonylation	0.07	0.32	0.40
GSTA4	—	0.80*	0.85**
ALDH2		—	0.96***

ALDH2, acetaldehyde dehydrogenase 2; FALDH, fatty aldehyde dehydrogenase; GSTA4, glutathione S-transferase A4.

* $P < 0.05$,

** $P < 0.01$,

*** $P < 0.001$.